Advances of MXenes

Subjects: Chemistry, Analytical | Medicine, Research & Experimental

Contributor: Aneesh Koyappayil, Sachin Ganpat Chavan, Yun-Gil Roh, Min-Ho Lee

MXenes are synthesized from ‘MAX’ phases by the selective etching of ‘A’ layers. The MAX phases are conductive 2D layers of transition metal carbides/nitrides interconnected by the ‘A’ element with strong ionic, metallic, and covalent bonds.

Keywords: MXene ; 2D materials ; biomedical applications

1. Introduction

Research on 2D materials can be traced back to the pioneering work of Langmuir on elemental monolayers in the 1930s [1]. The long-forgotten research area underwent a reawakening with the discovery of graphene, the first two-dimensional atomic crystal, in 2004 [2][3], and its profound success thereafter. Since then, 2D materials such as hexagonal boron nitride, transition metal dichalcogenides, phosphorenes, etc. have been discovered and explored for promising applications [4]. MXenes (pronounced ‘maxenes’) emerged as an elegant member of the above category and soon proved to be versatile enough to revolutionize many aspects of human life by replacing some of the commonly used 2D materials to become the next disruptive technology. MXenes are synthesized from ‘MAX’ phases by the selective etching of ‘A’ layers. The MAX phases are conductive 2D layers of transition metal carbides/nitrides interconnected by the ‘A’ element with strong ionic, metallic, and covalent bonds [5]. As shown in **Figure 1**, a typical MXene 2D flake is formed by transition elements such as Sc, Ti, V, Cr, Mn, Fe, Y, Zr, Nb, Mo, Hf, Ta, and W interleaved by carbon or nitrogen with the general formula $M_{n+1}X_nT_x$, where T_x represents surface functionalities such as F, Cl, O, and OH [6][7][8]. The history of MXenes begins in the year 2011 with the synthesis of 2D-layered $Ti_3C_2T_x$ from the exfoliation of Ti_3AlC_2 MAX phase by Gogotsi‘s group [9]. The initial synthesis approach was conceptualized based on the weak Ti-Al metallic bond. This enabled the easy removal of Al atoms from the Ti_3AlC_2 MAX phase, such as AlF_3, which was later removed by simple washing and resulted in a multilayered, accordion-like structure. This etching process was widely explored for the synthesis of different MXenes, and parameters such as etching time and HF concentration were optimized [10][11]. Owing to the high risk in handling and the corrosive nature of HF, several lower-risk alternative approaches have been conceptualized. Some of these approaches involved chemicals or combinations of chemicals such as NH_4HF_2 [12], HCl/FeF_3 [13], HCl/LiF [14], HCl/NaF [15], HCl/KF [16], HCl/NH_4F/KF [17], and HCl/NH_4F [18], which can act as an in situ source of fluoride ions and improve the safety in operation to a large extent. Nowadays, fluorine-free synthesis approaches are gaining momentum as a new, safer gateway to MXene synthesis, and many innovative top-down synthesis routes, such as electrochemical etching [19] [20], thermally assisted electrochemical approaches [21], hydrothermal treatments in NaOH [22] and KOH solutions [23], element replacement by reaction with Lewis acid molten salts [24], salt-templated approaches [25], etc., have been introduced. Moreover, bottom-up synthesis by chemical vapor deposition (CVD), plasma-enhanced pulsed laser deposition (PEPLD), and template methods [26][27] were also reported for the synthesis of MXenes. Because of their 2D planar structure, hydrophilicity, endless and flexible functionalization possibilities, strong absorption in the near-infrared (NIR) region, and exceptional properties, biomedical applications emerged as one of the most promising application fields of MXenes (**Scheme 1**). MXenes are found to be suitable candidates for applications including anticancer and drug delivery, antimicrobial, photothermal therapy, biosensors, and tissue engineering. However, even with intensive research efforts on MXene, the outstanding properties of these materials alone still cannot meet all the requirements of various biomedical applications. To endow new functions and to improve the performance, MXenes were functionalized, and their surfaces modified. Recently, functional modification of MXenes and the combination of MXenes with 3D [28], 2D [29], 1D [30], 0D [31], and polymer materials [32] with covalent and non-covalent modifications opened a new horizon for the functional requirements of biomedical applications. MXenes were modified with heteroatoms such as sulfur [33], phosphorous [34], and nitrogen [35] to produce functional MXenes. Apart from this, MXenes with enhanced properties were synthesized by doping with boron [36], platinum [37], niobium [38], silicon and germanium [39], vanadium [40], and alkali and alkaline earth metal cations [41]. As an ideal biomaterial for biomedical applications, MXenes, and their composites could be engineered with different physical, mechanical, or chemical properties [42], and must be compatible with the physiological environment with reliable mechanical strength, degradability, and the ability to overcome biological rejection

[43]. Even though they have been less explored, several MXenes and their composites have proven to be biocompatible and non-toxic to living organisms [44], and MXenes such as niobium carbide have proven to be biodegradable in mice [45], thereby proving promising for in vivo applications.

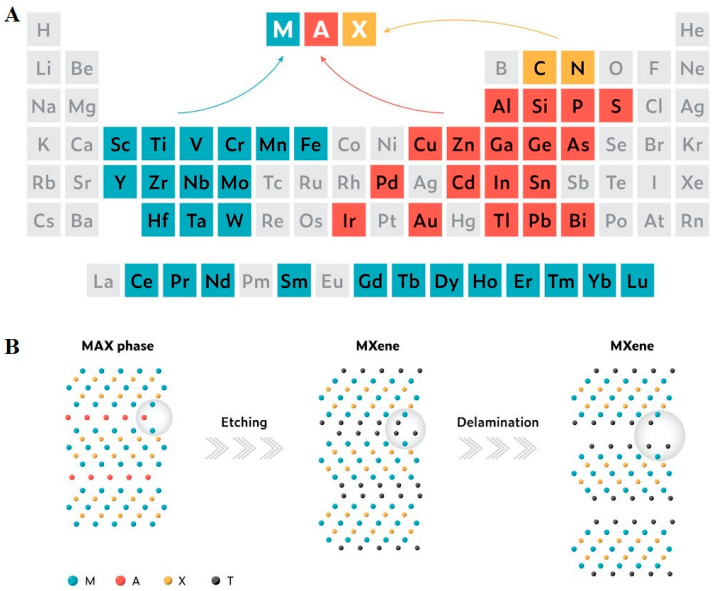

Figure 1. (**A**) The periodic table highlighting the 'M', 'A', and 'X' elements of known MAX phases. (**B**) Schematic illustration of the synthesis of MXenes from MAX phases. Reprinted with permission from Ref. [46]. Copyright © 2022 Wiley.

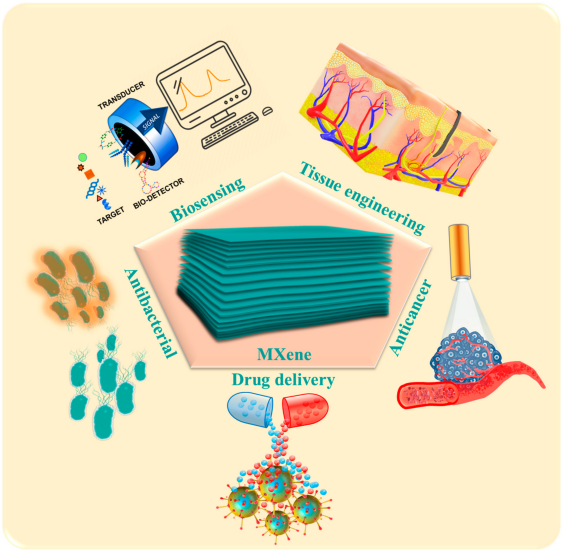

Scheme 1. Biomedical applications of MXenes.

2. Drug Delivery Applications

The unique 2D planar structure and physicochemical properties of MXenes make them favorable for precision drug delivery applications [47]. $Ti_3C_2T_x$, a prominent member of the MXene family, is renowned for its drug delivery applications (**Table 1**) because of its ultrathin planar nanostructure, excellent photothermal conversion capability, excellent near-infrared (NIR) responsiveness, and the chemically tunable nature of the surface functionalities [48][49][50]. An ideal drug delivery system requires controllability and sufficient drug-loading capability so that the drug-carrying nanovehicles continuously stay in the required body part. However, $Ti_3C_2T_x$-based nanovehicles lack sufficient controllability and suffer low drug-loading capability, so that, with blood circulation, the drug-carrying nanovehicles are continuously removed from the body site of application and cause inevitable damage to normal tissue [51]. Similar to other inorganic 2D materials, MXene-based nanoplatforms suffer stability in physiological conditions [52], which may affect the controllable release of the drug for cancer therapy. Therefore, fabricating a smart MXene-based nanoplatform for drug delivery remained a challenge. Controllability of a MXene-based drug carrier may be improved by adding magnetic nanomaterials so that the drug carrier could be controlled and confined to the target cells by the application of an external magnetic field. The drug, then, will be released by an endogenous or exogenous stimulation [53].

Table 1. Literature reports of MXenes for drug delivery applications.

MXene-Based Drug Carrier	Stimuli for Drug Release	Drug	Advantages	Ref.
$Ti_3C_2T_x$-SP	pH, NIR	Doxorubicin	High drug-loading capability of 211.8%.	[47]
$Ti_3C_2T_x$-CoNWs	pH, NIR	Doxorubicin	High drug-loading capacity of 225.05%.	[49]
$Ti_3C_2T_x$@GNRs/PDA/$Ti_3C_2T_x$	NIR	Doxorubicin	95.88% drug-loading ability.	[50]
$Ti_3C_2T_x$/Polyacrylamide	pH	Chloramphenicol	$Ti_3C_2T_x$/Polyacrylamide hydrogels exhibited a high drug-loading of 97.5–127.7 mg/g and drug release percentages of 62.1–81.4%.	[53]
HAP/CS/HA/MXene/AuNRs	pH, NIR	Doxorubicin	Drug encapsulation efficiency of 83.9%	[54]
Polymer-coated MXene nanobelt fibers	NIR	Vitamin E	NIR-induced relaxation of the interface by the polymeric coating layer to dissolve and release Vitamin E.	[55]
$Ti_3C_2T_x$@Agarose hydrogel	NIR	Doxorubicin	The DOX-loaded MXene-hydrogel exhibited rapid DOX release under NIR the irradiation, while almost no DOX release when NIR was turned off, proving an NIR switch for controlled drug release.	[56]
MXene@Agarose	NIR	HGF	Flexible and controllable release of the protein drugs with high precision.	[57]
MXenes-FA-SP	pH	Doxorubicin	Drug-loading capacity of 69.9% and 48 h long drug release time.	[58]
$Ti_3C_2T_x$@Met@CP	pH, NIR	Metformin	The functionalized $Ti_3C_2T_x$ nanosheets in the composite exhibited effective singlet oxygen generation, strong NIR absorption, and high photothermal conversion efficiency of ~59.6%.	[59]
Ti_2N@oSi	NIR	Doxorubicin	Ultrahigh drug-loading capacity of 796.3%.	[60]
MXene@MOF-5@DOX	pH	Doxorubicin/pCRISPR	Achieved a drug payload of 35.7%.	[61]

Note: The Ti_3C_2Tx MXene, also referred to as Ti_3C_2 or Ti_3C_2Tz is unified by the term Ti_3C_2Tx in the main text to avoid confusion.

3. Antimicrobial Applications

Microbial growth is considered a serious health concern. Among various 2D materials, MXenes (particularly $Ti_3C_2T_x$) have emerged as a promising candidate, showing antimicrobial activity even higher than graphene oxide [62]. MXenes have shown enhanced antimicrobial activity because of the enhanced cell membrane permeability, membrane rupture, DNA destruction because of the sharp edges, hydrophilicity, and hydrogen bonding with the cell membrane lipopolysaccharide molecules [63]. MXenes and their composites have shown excellent antibacterial properties against *Escherichia coli*, *Bacillus subtilis*, *Staphylococcus aureus*, *Pseudomonas aeruginosa*, and *Shigella* (**Table 2**). MXene functional groups are also reported to cause cell inactivation by preventing the intake of nutrients and thereby inhibiting the growth of bacteria [64]. The atomic structures of MXenes have been reported to have a crucial role in the antimicrobial properties of MXene [65]. Some MXenes such as $Ti_3C_2T_x$ and $TiVCT_x$ are reported to possess inherent antimicrobial properties. Additionally, the transfer of reactive electrons caused by the formation of a conductive bridge over the lipid bilayer from the bacterial cell to the external environment enables ultimate cell death [64]. Among the various other factors influencing the antibacterial efficiency of MXenes, environmental conditions and the structure of bacterial cell walls play a crucial role. Environmental conditions contribute to the aging of the membrane, and surface oxidation of $Ti_3C_2T_x$ in the air results in the formation of nanocrystals of anatase TiO_2 [66]. The TiO_2 catalyzed free radical formation enhances the antibacterial property of $Ti_3C_2T_x$ by stimulating oxidative stress on bacterial cell walls [66]. Since peptidoglycan thickness varies in gram-negative and gram-positive bacteria (peptidoglycan is thin in *E. coli* [67] and thick in *B. subtilis* [68]), a corresponding difference is observed in the resistance towards the MXene. Recently, the stoichiometry of the MXenes with the same chemical composition was also reported to exert considerable influence on its antibacterial activity [65].

Table 2. Literature reports on the antimicrobial applications of MXene/Composites.

MXene/Composite	Antimicrobial Applications	Ref.
$Ti_3C_2T_x$	Antibacterial activity against *E. coli* and *B. subtilis* with 98% viability loss within 4 h.	[62]
Colloidal $Ti_3C_2T_x$	Antibacterial activity against *B. subtilis* and *E. coli.*	[63]
$Ti_3C_2T_x$	Antibacterial activity against *E. coli.*	[65]
$Ti_3C_2T_x$	Photocatalytic inactivation of airborne *E. coli.*	[69]
$Bi_2S_3/Ti_3C_2T_x$	Photoexcited antimicrobial effects on *S. aureus* and *E. coli.*	[70]
$Ti_3C_2T_z$/Chitosan	Antibacterial activity against *E. coli* and *S. aureus.*	[71]
Nb_2CT_x and $Nb_4C_3T_x$	Bactericidal property against *E. coli* and *S. aureus.*	[72]
$Cu_2O/Ti_3C_2T_x$	Antibacterial activity against *S. aureus* and *Pseudomonas aeruginosa.*	[73]
$Ti_3C_2T_x$-AuNCs	Antibacterial performance on *S. aureus* and *E. coli.*	[74]
$MoS_2/Ti_3C_2T_x$	Antibacterial activity against *E. coli* and *B. subtilis.*	[75]
$Ti_3C_2T_x$-Laden bacteriophage	Antibacterial activity against *Shigella.*	[76]
$Ag/Ti_3C_2T_x$	Inhibitory activity against *E. coli* and *S. aureus.*	[77]
$TiVCT_X$	Antibacterial activities against *E. coli*, photothermal sterilization effect on *E. coli* and *B. subtilis.*	[78]
CuP-s$Ti_3C_2T_x$	Antibacterial activity against *E. coli* and *S. aureus.*	[79]
$Ti_3C_2T_x$	Size-dependent photothermal antibacterial activity against *S. aureus.*	[80]
$Ti_3C_2T_x$/PVA hydrogel	Antibacterial activity against *E. coli* and *S. aureus.*	[81]
V_2C NSs	Antibacterial activity against *E. coli*, and *B. subtilis.*	[82]
BC/Chi/$Ti_3C_2T_x$/AgNWs aerogel	Antibacterial activity against *E. coli* and *S. aureus.*	[83]

References

1. The Collected Works of Irving Langmuir: Surface Phenomena; Published with the Editorial Assistance of the General El ectric Company by Pergamon Press; Pergamon Press: Oxford, UK, 1961; Volume 9.
2. Geim, A.K.; Novoselov, K.S. The rise of graphene. In Nanoscience and Technology; Macmillan Publishers Ltd.: London, UK, 2009; pp. 11–19.
3. Novoselov, K.S.; Fal'ko, V.I.; Colombo, L.; Gellert, P.R.; Schwab, M.G.; Kim, K. A roadmap for graphene. Nature 2012, 490, 192–200.
4. Akinwande, D.; Brennan, C.J.; Bunch, J.S.; Egberts, P.; Felts, J.R.; Gao, H.; Huang, R.; Kim, J.-S.; Li, T.; Li, Y.; et al. A r eview on mechanics and mechanical properties of 2D materials—Graphene and beyond. Extrem. Mech. Lett. 2017, 13, 42–77.
5. Naguib, M.; Mochalin, V.N.; Barsoum, M.W.; Gogotsi, Y. 25th Anniversary Article: MXenes: A New Family of Two-Dimen sional Materials. Adv. Mater. 2014, 26, 992–1005.
6. Gogotsi, Y.; Anasori, B. The Rise of MXenes. ACS Nano 2019, 13, 8491–8494.
7. Ihsanullah, I. MXenes as next-generation materials for the photocatalytic degradation of pharmaceuticals in water. J. E nviron. Chem. Eng. 2022, 10, 107381.
8. Huang, K.; Li, Z.; Lin, J.; Han, G.; Huang, P. Two-dimensional transition metal carbides and nitrides (MXenes) for biome dical applications. Chem. Soc. Rev. 2018, 47, 5109–5124.
9. Naguib, M.; Kurtoglu, M.; Presser, V.; Lu, J.; Niu, J.; Heon, M.; Hultman, L.; Gogotsi, Y.; Barsoum, M.W. Two-Dimension al Nanocrystals Produced by Exfoliation of Ti3AlC2. Adv. Mater. 2011, 23, 4248–4253.
10. Naguib, M.; Mashtalir, O.; Carle, J.; Presser, V.; Lu, J.; Hultman, L.; Gogotsi, Y.; Barsoum, M.W. Two-Dimensional Tran sition Metal Carbides. ACS Nano 2012, 6, 1322–1331.
11. Munir, S.; Rasheed, A.; Rasheed, T.; Ayman, I.; Ajmal, S.; Rehman, A.; Shakir, I.; Agboola, P.O.; Warsi, M.F. Exploring t he Influence of Critical Parameters for the Effective Synthesis of High-Quality 2D MXene. ACS Omega 2020, 5, 26845–

26854.

12. Halim, J.; Lukatskaya, M.R.; Cook, K.M.; Lu, J.; Smith, C.R.; Näslund, L.-Å.; May, S.J.; Hultman, L.; Gogotsi, Y.; Eklund, P.; et al. Transparent Conductive Two-Dimensional Titanium Carbide Epitaxial Thin Films. Chem. Mater. 2014, 26, 2374–2381.
13. Wang, X.; Garnero, C.; Rochard, G.; Magne, D.; Morisset, S.; Hurand, S.; Chartier, P.; Rousseau, J.; Cabioc'h, T.; Coutanceau, C. A new etching environment (FeF3/HCl) for the synthesis of two-dimensional titanium carbide MXenes: A route towards selective reactivity vs. water. J. Mater. Chem. A 2017, 5, 22012–22023.
14. Ghidiu, M.; Lukatskaya, M.R.; Zhao, M.-Q.; Gogotsi, Y.; Barsoum, M.W. Conductive two-dimensional titanium carbide 'clay'with high volumetric capacitance. Nature 2014, 516, 78–81.
15. Wu, M.; Wang, B.; Hu, Q.; Wang, L.; Zhou, A. The Synthesis Process and Thermal Stability of V2C MXene. Materials 2018, 11, 2112.
16. Wang, L.; Liu, D.; Lian, W.; Hu, Q.; Liu, X.; Zhou, A. The preparation of V2CTx by facile hydrothermal-assisted etching processing and its performance in lithium-ion battery. J. Mater. Res. Technol. 2020, 9, 984–993.
17. Liu, F.; Zhou, A.; Chen, J.; Jia, J.; Zhou, W.; Wang, L.; Hu, Q. Preparation of Ti3C2 and Ti2C MXenes by fluoride salts etching and methane adsorptive properties. Appl. Surf. Sci. 2017, 416, 781–789.
18. Kvashina, T.S.; Uvarov, N.F.; Korchagin, M.A.; Krutskiy, Y.L.; Ukhina, A.V. Synthesis of MXene Ti3C2 by selective etching of MAX-phase Ti3AlC2. Mater. Today Proc. 2020, 31, 592–594.
19. Sun, W.; Shah, S.A.; Chen, Y.; Tan, Z.; Gao, H.; Habib, T.; Radovic, M.; Green, M.J. Electrochemical etching of Ti2AlC to Ti2CTx (MXene) in low-concentration hydrochloric acid solution. J. Mater. Chem. A 2017, 5, 21663–21668.
20. Li, X.; Li, M.; Yang, Q.; Liang, G.; Huang, Z.; Ma, L.; Wang, D.; Mo, F.; Dong, B.; Huang, Q. In situ electrochemical synthesis of MXenes without Acid/Alkali usage in/for an aqueous zinc ion battery. Adv. Energy Mater. 2020, 10, 2001791.
21. Pang, S.-Y.; Wong, Y.-T.; Yuan, S.; Liu, Y.; Tsang, M.-K.; Yang, Z.; Huang, H.; Wong, W.-T.; Hao, J. Universal strategy for HF-free facile and rapid synthesis of two-dimensional MXenes as multifunctional energy materials. J. Am. Chem. Soc. 2019, 141, 9610–9616.
22. Li, T.; Yao, L.; Liu, Q.; Gu, J.; Luo, R.; Li, J.; Yan, X.; Wang, W.; Liu, P.; Chen, B. Fluorine-free synthesis of high-purity Ti3C2Tx (T = OH, O) via alkali treatment. Angew. Chem. Int. Ed. 2018, 57, 6115–6119.
23. Li, G.; Tan, L.; Zhang, Y.; Wu, B.; Li, L. Highly efficiently delaminated single-layered MXene nanosheets with large lateral size. Langmuir 2017, 33, 9000–9006.
24. Li, M.; Lu, J.; Luo, K.; Li, Y.; Chang, K.; Chen, K.; Zhou, J.; Rosen, J.; Hultman, L.; Eklund, P. Element replacement approach by reaction with Lewis acidic molten salts to synthesize nanolaminated MAX phases and MXenes. J. Am. Chem. Soc. 2019, 141, 4730–4737.
25. Urbankowski, P.; Anasori, B.; Hantanasirisakul, K.; Yang, L.; Zhang, L.; Haines, B.; May, S.J.; Billinge, S.J.L.; Gogotsi, Y. 2D molybdenum and vanadium nitrides synthesized by ammoniation of 2D transition metal carbides (MXenes). Nanoscale 2017, 9, 17722–17730.
26. Xu, C.; Wang, L.; Liu, Z.; Chen, L.; Guo, J.; Kang, N.; Ma, X.-L.; Cheng, H.-M.; Ren, W. Large-area high-quality 2D ultrathin Mo2C superconducting crystals. Nat. Mater. 2015, 14, 1135–1141.
27. Xu, C.; Chen, L.; Liu, Z.; Cheng, H.-M.; Ren, W. Bottom-up synthesis of 2D transition metal carbides and nitrides. In 2D Metal Carbides and Nitrides (MXenes); Springer: Cham, Switzerland, 2019; pp. 89–109.
28. Xu, Y.; Zhang, K.; Chen, S.; Zhang, X.; Chen, Y.; Li, D.; Xu, F. Two-dimensional lamellar MXene/three-dimensional network bacterial nanocellulose nanofiber composite Janus membranes as nanofluidic osmotic power generators. Electrochim. Acta 2022, 412, 140162.
29. Dwivedi, N.; Dhand, C.; Kumar, P.; Srivastava, A.K. Emergent 2D materials for combating infectious diseases: The potential of MXenes and MXene–graphene composites to fight against pandemics. Mater. Adv. 2021, 2, 2892–2905.
30. Wang, X.; Luo, D.; Wang, J.; Sun, Z.; Cui, G.; Chen, Y.; Wang, T.; Zheng, L.; Zhao, Y.; Shui, L. Strain engineering of a MXene/CNT hierarchical porous hollow microsphere electrocatalyst for a high-efficiency lithium polysulfide conversion process. Angew. Chem. Int. Ed. 2021, 60, 2371–2378.
31. Cao, B.; Liu, H.; Zhang, X.; Zhang, P.; Zhu, Q.; Du, H.; Wang, L.; Zhang, R.; Xu, B. MOF-Derived ZnS Nanodots/Ti3C2Tx MXene Hybrids Boosting Superior Lithium Storage Performance. Nano-Micro Lett. 2021, 13, 202.
32. Wang, B.; Lai, X.; Li, H.; Jiang, C.; Gao, J.; Zeng, X. Multifunctional MXene/chitosan-coated cotton fabric for intelligent fire protection. ACS Appl. Mater. Interfaces 2021, 13, 23020–23029.
33. Zhang, Y.; Li, J.; Gong, Z.; Xie, J.; Lu, T.; Pan, L. Nitrogen and sulfur co-doped vanadium carbide MXene for highly reversible lithium-ion storage. J. Colloid Interface Sci. 2021, 587, 489–498.

34. Yoon, Y.; Tiwari, A.P.; Choi, M.; Novak, T.G.; Song, W.; Chang, H.; Zyung, T.; Lee, S.S.; Jeon, S.; An, K.S. Precious-Metal-Free Electrocatalysts for Activation of Hydrogen Evolution with Nonmetallic Electron Donor: Chemical Composition Controllable Phosphorous Doped Vanadium Carbide MXene. Adv. Funct. Mater. 2019, 29, 1903443.

35. Liu, R.; Cao, W.; Han, D.; Mo, Y.; Zeng, H.; Yang, H.; Li, W. Nitrogen-doped Nb2CTx MXene as anode materials for lithium ion batteries. J. Alloys Compd. 2019, 793, 505–511.

36. Zheng, S.; Li, S.; Mei, Z.; Hu, Z.; Chu, M.; Liu, J.; Chen, X.; Pan, F. Electrochemical nitrogen reduction reaction performance of single-boron catalysts tuned by MXene substrates. J. Phys. Chem. Lett. 2019, 10, 6984–6989.

37. Kan, D.; Wang, D.; Zhang, X.; Lian, R.; Xu, J.; Chen, G.; Wei, Y. Rational design of bifunctional ORR/OER catalysts based on Pt/Pd-doped Nb2CT2 MXene by first-principles calculations. J. Mater. Chem. A 2020, 8, 3097–3108.

38. Fatima, M.; Fatheema, J.; Monir, N.B.; Siddique, A.H.; Khan, B.; Islam, A.; Akinwande, D.; Rizwan, S. Nb-doped MXene with enhanced energy storage capacity and stability. Front. Chem. 2020, 8, 168.

39. Balcı, E.; Akkuş, Ü.Ö.; Berber, S. Doped Sc2C(OH)2 MXene: New type s-pd band inversion topological insulator. J. Phys. Condens. Matter 2018, 30, 155501.

40. Gao, Z.W.; Zheng, W.; Lee, L.Y.S. Highly Enhanced Pseudocapacitive Performance of Vanadium-Doped MXenes in Neutral Electrolytes. Small 2019, 15, 1902649.

41. Huang, W.; Hu, L.; Tang, Y.; Xie, Z.; Zhang, H. Recent Advances in Functional 2D MXene-Based Nanostructures for Next-Generation Devices. Adv. Funct. Mater. 2020, 30, 2005223.

42. Balakrishnan, P.; Thomas, S. Inert ceramics. In Fundamental Biomaterials: Ceramics; Elsevier: Amsterdam, The Netherlands, 2018; p. 117.

43. George, S.M.; Kandasubramanian, B. Advancements in MXene-Polymer composites for various biomedical applications. Ceram. Int. 2020, 46, 8522–8535.

44. Chen, K.; Qiu, N.; Deng, Q.; Kang, M.-H.; Yang, H.; Baek, J.-U.; Koh, Y.-H.; Du, S.; Huang, Q.; Kim, H.-E. Cytocompatibility of Ti3AlC2, Ti3SiC2, and Ti2AlN: In Vitro Tests and First-Principles Calculations. ACS Biomater. Sci. Eng. 2017, 3, 2293–2301.

45. Lin, H.; Gao, S.; Dai, C.; Chen, Y.; Shi, J. A Two-Dimensional Biodegradable Niobium Carbide (MXene) for Photothermal Tumor Eradication in NIR-I and NIR-II Biowindows. J. Am. Chem. Soc. 2017, 139, 16235–16247.

46. Wang, Y.; Guo, T.; Tian, Z.; Bibi, K.; Zhang, Y.-Z.; Alshareef, H.N. MXenes for Energy Harvesting. Adv. Mater. 2022, 34, 2108560.

47. Han, X.; Huang, J.; Lin, H.; Wang, Z.; Li, P.; Chen, Y. 2D Ultrathin MXene-Based Drug-Delivery Nanoplatform for Synergistic Photothermal Ablation and Chemotherapy of Cancer. Adv. Healthc. Mater. 2018, 7, 1701394.

48. Lin, H.; Wang, X.; Yu, L.; Chen, Y.; Shi, J. Two-Dimensional Ultrathin MXene Ceramic Nanosheets for Photothermal Conversion. Nano Lett. 2017, 17, 384–391.

49. Liu, Y.; Han, Q.; Yang, W.; Gan, X.; Yang, Y.; Xie, K.; Xie, L.; Deng, Y. Two-dimensional MXene/cobalt nanowire heterojunction for controlled drug delivery and chemo-photothermal therapy. Mater. Sci. Eng. C 2020, 116, 111212.

50. Zhu, B.; Shi, J.; Liu, C.; Li, J.; Cao, S. In-situ self-assembly of sandwich-like Ti3C2 MXene/gold nanorods nanosheets for synergistically enhanced near-infrared responsive drug delivery. Ceram. Int. 2021, 47, 24252–24261.

51. Xu, B.; Zhi, C.; Shi, P. Latest advances in MXene biosensors. J. Phys. Mater. 2020, 3, 031001.

52. Iqbal, A.; Hong, J.; Ko, T.Y.; Koo, C.M. Improving oxidation stability of 2D MXenes: Synthesis, storage media, and conditions. Nano Converg. 2021, 8, 9.

53. Zhang, P.; Yang, X.-J.; Li, P.; Zhao, Y.; Niu, Q.J. Fabrication of novel MXene(Ti3C2)/polyacrylamide nanocomposite hydrogels with enhanced mechanical and drug release properties. Soft Matter 2020, 16, 162–169.

54. Wu, Z.; Shi, J.; Song, P.; Li, J.; Cao, S. Chitosan/hyaluronic acid based hollow microcapsules equipped with MXene/gold nanorods for synergistically enhanced near infrared responsive drug delivery. Int. J. Biol. Macromol. 2021, 183, 870–879.

55. Jin, L.; Guo, X.; Gao, D.; Wu, C.; Hu, B.; Tan, G.; Du, N.; Cai, X.; Yang, Z.; Zhang, X. NIR-responsive MXene nanobelts for wound healing. NPG Asia Mater. 2021, 13, 24.

56. Dong, Y.; Li, S.; Li, X.; Wang, X. Smart MXene/agarose hydrogel with photothermal property for controlled drug release. Int. J. Biol. Macromol. 2021, 190, 693–699.

57. Wang, S.; Zhang, Z.; Wei, S.; He, F.; Li, Z.; Wang, H.-H.; Huang, Y.; Nie, Z. Near-infrared light-controllable MXene hydrogel for tunable on-demand release of therapeutic proteins. Acta Biomater. 2021, 130, 138–148.

58. Liu, Z.; Xie, L.; Yan, J.; Liu, P.; Wen, H.; Liu, H. Folic Acid-Targeted MXene Nanoparticles for Doxorubicin Loaded Drug Delivery. Aust. J. Chem. 2021, 74, 847–855.

59. Bai, L.; Yi, W.; Sun, T.; Tian, Y.; Zhang, P.; Si, J.; Hou, X.; Hou, J. Surface modification engineering of two-dimensional t itanium carbide for efficient synergistic multitherapy of breast cancer. J. Mater. Chem. B 2020, 8, 6402–6417.

60. Li, L.; Lu, Y.; Qian, Z.; Yang, Z.; Zong, S.; Wang, Z.; Cui, Y. A Ti2N MXene-based nanosystem with ultrahigh drug loadin g for dual-strategy synergistic oncotherapy. Nanoscale 2021, 13, 18546–18557.

61. Rabiee, N.; Bagherzadeh, M.; Jouyandeh, M.; Zarrintaj, P.; Saeb, M.R.; Mozafari, M.; Shokouhimehr, M.; Varma, R.S. Natural Polymers Decorated MOF-MXene Nanocarriers for Co-delivery of Doxorubicin/pCRISPR. ACS Appl. Bio Mater. 2021, 4, 5106–5121.

62. Rasool, K.; Helal, M.; Ali, A.; Ren, C.E.; Gogotsi, Y.; Mahmoud, K.A. Antibacterial Activity of Ti3C2Tx MXene. ACS Nan o 2016, 10, 3674–3684.

63. Arabi Shamsabadi, A.; Sharifian Gh, M.; Anasori, B.; Soroush, M. Antimicrobial Mode-of-Action of Colloidal Ti3C2Tx MX ene Nanosheets. ACS Sustain. Chem. Eng. 2018, 6, 16586–16596.

64. Khatami, M.; Iravani, P.; Jamalipour Soufi, G.; Iravani, S. MXenes for antimicrobial and antiviral applications: Recent ad vances. Mater. Technol. 2021, 1–16.

65. Jastrzębska, A.M.; Karwowska, E.; Wojciechowski, T.; Ziemkowska, W.; Rozmysłowska, A.; Chlubny, L.; Olszyna, A. Th e Atomic Structure of Ti2C and Ti3C2 MXenes is Responsible for Their Antibacterial Activity toward E. coli Bacteria. J. Mater. Eng. Perform. 2019, 28, 1272–1277.

66. Peng, C.; Wang, H.; Yu, H.; Peng, F. (111) TiO2−x/Ti3C2: Synergy of active facets, interfacial charge transfer and Ti3+ doping for enhance photocatalytic activity. Mater. Res. Bull. 2017, 89, 16–25.

67. Huang, K.C.; Mukhopadhyay, R.; Wen, B.; Gitai, Z.; Wingreen, N.S. Cell shape and cell-wall organization in Gram-nega tive bacteria. Proc. Natl. Acad. Sci. USA 2008, 105, 19282–19287.

68. Tocheva, E.I.; López-Garrido, J.; Hughes, H.V.; Fredlund, J.; Kuru, E.; Vannieuwenhze, M.S.; Brun, Y.V.; Pogliano, K.; J ensen, G.J. Peptidoglycan transformations during Bacillus subtilis sporulation. Mol. Microbiol. 2013, 88, 673–686.

69. Lu, S.; Meng, G.; Wang, C.; Chen, H. Photocatalytic inactivation of airborne bacteria in a polyurethane foam reactor loa ded with a hybrid of MXene and anatase TiO2 exposing facets. Chem. Eng. J. 2021, 404, 126526.

70. Li, J.; Li, Z.; Liu, X.; Li, C.; Zheng, Y.; Yeung, K.W.K.; Cui, Z.; Liang, Y.; Zhu, S.; Hu, W.; et al. Interfacial engineering of Bi2S3/Ti3C2Tx MXene based on work function for rapid photo-excited bacteria-killing. Nat. Commun. 2021, 12, 1224.

71. Mayerberger, E.A.; Street, R.M.; McDaniel, R.M.; Barsoum, M.W.; Schauer, C.L. Antibacterial properties of electrospun Ti3C2Tz(MXene)/chitosan nanofibers. RSC Adv. 2018, 8, 35386–35394.

72. Pandey, R.P.; Rasheed, P.A.; Gomez, T.; Rasool, K.; Ponraj, J.; Prenger, K.; Naguib, M.; Mahmoud, K.A. Effect of Shee t Size and Atomic Structure on the Antibacterial Activity of Nb-MXene Nanosheets. ACS Appl. Nano Mater. 2020, 3, 113 72–11382.

73. Wang, W.; Feng, H.; Liu, J.; Zhang, M.; Liu, S.; Feng, C.; Chen, S. A photo catalyst of cuprous oxide anchored MXene nanosheet for dramatic enhancement of synergistic antibacterial ability. Chem. Eng. J. 2020, 386, 124116.

74. Zheng, K.; Li, S.; Jing, L.; Chen, P.-Y.; Xie, J. Synergistic Antimicrobial Titanium Carbide (MXene) Conjugated with Gold Nanoclusters. Adv. Healthc. Mater. 2020, 9, 2001007.

75. Alimohammadi, F.; Sharifian, M.; Attanayake, N.H.; Thenuwara, A.C.; Gogotsi, Y.; Anasori, B.; Strongin, D.R. Antimicrob ial Properties of 2D MnO2 and MoS2 Nanomaterials Vertically Aligned on Graphene Materials and Ti3C2 MXene. Lang muir 2018, 34, 7192–7200.

76. Mansoorianfar, M.; Shahin, K.; Hojjati-Najafabadi, A.; Pei, R. MXene–laden bacteriophage: A new antibacterial candidat e to control bacterial contamination in water. Chemosphere 2022, 290, 133383.

77. Zhu, X.; Zhu, Y.; Jia, K.; Abraha, B.S.; Li, Y.; Peng, W.; Zhang, F.; Fan, X.; Zhang, L. A near-infrared light-mediated anti microbial based on Ag/Ti3C2Tx for effective synergetic antibacterial applications. Nanoscale 2020, 12, 19129–19141.

78. He, Q.; Hu, H.; Han, J.; Zhao, Z. Double transition-metal TiVCTX MXene with dual-functional antibacterial capability. M ater. Lett. 2022, 308, 131100.

79. Liu, L.; Zhu, M.; Ma, Z.; Xu, X.; Mohesen Seraji, S.; Yu, B.; Sun, Z.; Wang, H.; Song, P. A reactive copper-organophosp hate-MXene heterostructure enabled antibacterial, self-extinguishing and mechanically robust polymer nanocomposite s. Chem. Eng. J. 2022, 430, 132712.

80. Gao, Y.; Dong, Y.; Yang, S.; Mo, A.; Zeng, X.; Chen, Q.; Peng, Q. Size-dependent photothermal antibacterial activity of Ti3C2Tx MXene nanosheets against methicillin-resistant Staphylococcus aureus. J. Colloid Interface Sci. 2022, 617, 53 3–541.

81. Li, Y.; Han, M.; Cai, Y.; Jiang, B.; Zhang, Y.; Yuan, B.; Zhou, F.; Cao, C. Muscle-inspired MXene/PVA hydrogel with high toughness and photothermal therapy for promoting bacteria-infected wound healing. Biomater. Sci. 2022, 10, 1068–1082.
82. Zada, S.; Lu, H.; Yang, F.; Zhang, Y.; Cheng, Y.; Tang, S.; Wei, W.; Qiao, Y.; Fu, P.; Dong, H.; et al. V2C Nanosheets as Dual-Functional Antibacterial Agents. ACS Appl. Bio Mater. 2021, 4, 4215–4223.
83. Fu, Y.; Cheng, Y.; Wei, Q.; Zhao, Y.; Zhang, W.; Yang, Y.; Li, D. Multifunctional Biomass Composite Aerogel Co-Modified by MXene and Ag Nanowires for Health Monitoring and Synergistic Antibacterial Applications. Appl. Surf. Sci. 2022, 598, 153783.